Eur. Phys. J. C 23, 185–190 (2002)
Digital Object Identifier (DOI) 10.1007/s100520100861

THE EUROPEAN PHYSICAL JOURNAL C

Implications of the pseudo-scalar Higgs boson in determining the neutralino dark matter

A.B. Lahanas[1], V.C. Spanos[2]

[1] University of Athens, Physics Department, Nuclear and Particle Physics Section, 15771 Athens, Greece
[2] Institut für Hochenergiephysik der Österreichischen Akademie der Wissenschaften, 1050 Vienna, Austria

Received: 22 July 2001 / Revised version: 13 November 2001 /
Published online: 18 January 2002 –

Abstract. In the framework of the constrained minimal supersymmetric standard model (CMSSM) we discuss the impact of the pseudo-scalar Higgs boson in delineating regions of the parameters which are consistent with cosmological data and E821 data on the anomalous magnetic moment of the muon. For the large values of the parameter $\tan\beta > 50$, cosmologically allowed corridors of large m_0, $M_{1/2}$ are opened, due to the s-channel pseudo-scalar exchange in the pair annihilation of the lightest of the neutralinos to $b\bar{b}$ or $\tau\bar{\tau}$, which dominates in this region. However, no such corridors are found for values $\tan\beta < 50$. Combining cosmological and E821 data puts severe upper limits on the sparticle masses. We find that at LHC, but even at a e^+e^- linear collider with center of mass energy $s^{1/2} = 800\,\mathrm{GeV}$, such as TESLA, supersymmetry can be discovered, if it is based on the CMSSM.

1 Introduction

In the framework of supersymmetric models with R-parity conservation, it has been argued that for large $\tan\beta$ the neutralino relic density ($\Omega_{\tilde{\chi}}h_0^2$) can be compatible with the recent cosmological data which favor small values for $\Omega_{\tilde{\chi}}h_0^2$. In this regime the neutralino ($\tilde{\chi}$) pair annihilation through s-channel pseudo-scalar Higgs boson (A) exchange leads to enhanced annihilation cross sections reducing significantly the relic density [1], while the heavy CP-even Higgs (H) exchange is P-wave suppressed and not that important. The importance of this mechanism, in conjunction with the recent cosmological data which favor small values of the dark matter (DM) relic density, has been stressed in [2]. The same mechanism has also been invoked in [3,4], where it has been shown that it enlarges the cosmologically allowed regions. In fact cosmology does not put severe upper bounds on the sparticle masses, and soft masses can be in the TeV region, pushing up the sparticle mass spectrum to regions that might escape detection in future planned accelerators. Such upper bounds are imposed, however, by the recent $g-2$ E281 data [5] constraining the CMSSM in such a way that supersymmetry will be accessible to LHC or other planned e^+e^- linear colliders if their center of mass energy is larger than about 1.2 TeV [6]. The bounds put by $g-2$ has been the subject of intense phenomenological study [6–9], and although the situation has not been definitely settled, supersymmetry emerges as a prominent candidate in explaining the discrepancy between the standard model predictions and experimental measurements.

In this study we undertake the problem of calculating the neutralino relic density, in the framework of the CMSSM, paying special attention to the pseudo-scalar Higgs exchange which dominates in the large $\tan\beta$ region. In this regime the cosmologically allowed domains depend sensitively on this mechanism and in conjunction with the bounds put by the $g-2$ measurements can severely constrain the CMSSM predictions. In particular, we find that cosmologically allowed corridors of large $m_0, M_{1/2}$ values open up for $\tan\beta > 50$, which however have little overlap with the regions allowed by the E821 data. The constraints imposed on the sparticle spectrum and the potential of discovering CMSSM in future accelerators are discussed.

2 The role of the pseudo-scalar Higgs boson mass

The $\tilde{\chi}\tilde{\chi}$ fusion to the pseudo-scalar Higgs boson, A, which subsequently decays to a $b\bar{b}$ or a $\tau\bar{\tau}$, becomes the dominant annihilation mechanism for large $\tan\beta$ when the pseudo-scalar mass m_A approaches twice the neutralino mass, $m_A \simeq 2m_{\tilde{\chi}}$. In fact, by increasing $\tan\beta$ the mass m_A decreases, while the neutralino mass remains almost constant, if the other parameters are kept fixed. Thus m_A is expected eventually to enter into the regime in which it is close to the pole value $m_A = 2m_{\tilde{\chi}}$, and the pseudo-scalar Higgs exchange dominates. It is interesting to point out that in a previous analysis of the direct DM searches [10], we had stressed that the contribution of the CP-even Higgs bosons exchange to the LSP–nucleon scatter-

ing cross sections increases with $\tan\beta$. Therefore in the large $\tan\beta$ regime one obtains the highest possible rates for the direct DM searches. Similar results are presented in [11].

In the framework of the CMSSM the chargino mass bound as well as the recent LEP Higgs mass bound [12] already exclude regions in which $\tilde{\chi}$ has a large Higgsino component, and thus in the regions of interest the $\tilde{\chi}$ is mainly a bino. A bino is characterized by a very small coupling to the pseudo-scalar Higgs A; however, the magnitude of $\tan\beta$ balances the smallness of its coupling giving a sizeable effect when $m_A \simeq 2m_{\tilde{\chi}}$, making s-channel pseudo-scalar exchange important.

It becomes obvious from the previous discussion that an unambiguous and reliable determination of the A-mass, m_A, is demanded before one embarks on calculating the neutralino relic density especially in regions where the s-channel pseudo-scalar exchange dominates. In the constrained SUSY models, such as the CMSSM, m_A is not a free parameter but is determined once m_0, $M_{1/2}$ and A as well as $\tan\beta$ and the sign of μ, sign(μ), are given. m_A depends sensitively on the Higgs mixing parameter, m_3^2, which is determined from minimizing the one-loop corrected effective potential. A subtlety arises for large $\tan\beta$ values since the corrections are relatively large mainly due to the smallness of the Higgs mixing parameter. In order to handle this we calculate the effective potential using as reference scale the average stop scale $Q_{\tilde{t}} \simeq (m_{\tilde{t}_1} m_{\tilde{t}_2})^{1/2}$ [13]. At this scale the contributions of the third generation sfermions are small. However, other contributions may not be negligible at this scale and should be properly taken into account. In particular, the neutralino and chargino contributions to the effective potential should be included for a more reliable calculation. These do not vanish at $Q_{\tilde{t}}$ since their masses, determined by the gaugino masses M_1, M_2 and the μ value, may be quite different from $Q_{\tilde{t}}$. Their inclusion to the effective potential improves the mass of the A-Higgs, as this is calculated from the effective potential, yielding a result that is scale independent and approximates the pole mass to better than 2% if we also include the scale dependent logarithmic contributions from the wave function renormalization $\Pi(0) - \Pi(m_A^2)$ [14]. In the present work, for a more accurate determination of the pseudo-scalar Higgs we use the pole mass using the expression of [15].

A more significant correction, which drastically affects the pseudo-scalar mass, arises from the gluino–sbottom and chargino–stop corrections to the bottom quark Yukawa coupling [15–20]. Taking these effects into account the tree-level relation between the bottom mass and the corresponding Yukawa coupling is modified according to

$$m_b = v_1(h_b + \Delta h_b \tan\beta), \tag{1}$$

where Δh_b is

$$\frac{\Delta h_b}{h_b} = \frac{2\alpha_s}{3\pi} m_{\tilde{g}} \mu G(m^2_{\tilde{b}_1}, m^2_{\tilde{b}_2}, m^2_{\tilde{g}}) - \frac{h_t^2}{16\pi^2} \mu A_t G(m^2_{\tilde{t}_1}, m^2_{\tilde{t}_2}, \mu^2). \tag{2}$$

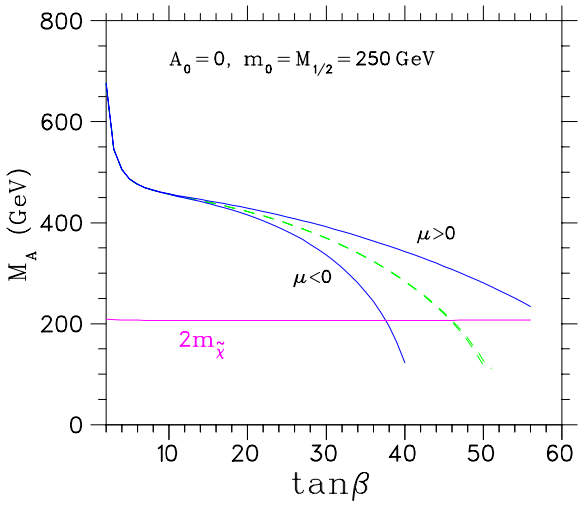

Fig. 1. The pseudo-scalar Higgs masses for $\mu > 0$ and $\mu < 0$ as a function of $\tan\beta$ (solid lines). The dashed lines are the same masses when the supersymmetric corrections to the bottom Yukawa coupling are ignored

In this the first (second) term is the gluino, sbottom (chargino, stop) corrections. In the second term we have ignored the small electroweak mixing effects. The function G in (2) is the one used in [18,17,20] which in [17] is denoted by I. It is known that the proper resummation of these corrections is important for a correct determination of h_b [19,20]. Equations (1) and (2) agree with those of [20] and therefore these corrections have been properly resummed[1].

These are very important, especially the SQCD corrections, and should be duly taken into account. The important point is that these affect differently the $\mu > 0$ and $\mu < 0$ values of m_A in a drastic way. In Fig. 1 we show the behavior for the pseudo-scalar Higgs boson mass as a function of the parameter $\tan\beta$ for the inputs shown in the figure, for both signs of μ, with and without the aforementioned corrections. Also plotted is the value of the quantity $2m_{\tilde{\chi}}$. One observes that in the absence of these correction to the bottom Yukawa coupling, the pseudo-scalar Higgs mass in the two cases differ little and meet the $2m_{\tilde{\chi}}$ line at $\tan\beta \simeq 40$. Obviously the $\tan\beta$ region around this value leads to enhanced neutralino annihilation cross sections through A-exchange since we are in the vicinity of a pole. However, when the aforementioned corrections are taken into account the values of the pseudo-scalar mass in the two cases split as shown in the figure. The one corresponding to $\mu > 0$ is moving upwards and that to $\mu < 0$ downwards. Thus only the second one can reach the pole value $2m_{\tilde{\chi}}$ at a smaller $\tan\beta$ however. The mass corresponding to $\mu > 0$ stays away from this, never reaching it, at least in the case shown, since for higher values of $\tan\beta$ we enter regions which are theoretically forbidden. Actually in these regions electroweak symmetry breaking does not occur. The $\mu < 0$ case does not stay comfortably well

[1] Our μ and the soft gaugino masses differ in sign from those of [17,20], while A_t has the same sign

with the $b \to s + \gamma$ process, as well as with the observed discrepancy of the $g-2$ data, if the latter are attributed to supersymmetry, and therefore we shall discard it in the sequel.

It is obvious from the previous discussion that the crucial parameter in this analysis is the ratio $m_A/2m_{\tilde{\chi}}$. The calculation of the pseudo-scalar Higgs boson mass m_A we have discussed in detail before. For the calculation of the $\tilde{\chi}$-mass we use the one-loop corrections of [15]. These result in corrections as large as 5%, in some cases, reducing the aforementioned ratio, driving it closer to the pole value.

3 Numerical results; discussion

Before embarking on a presention of our results we shall comment on the numerical analysis employed in this paper. This will be useful when comparing the results of this paper with those of other works, which use different numerical schemes in determining the mass parameters of the CMSSM. The predictions for the sparticle spectrum, including the mass of the pseudo-scalar Higgs, as well as the calculation of the relic density itself, may be sensitive to some of the parameters and the particular scheme employed.

In our analysis we use two-loop renormalization group equations (RGE's), in the $\overline{\rm DR}$ scheme, for all masses and couplings involved. The unification scale $M_{\rm GUT}$ is defined as the point at which the gauge couplings $\hat{\alpha}_1$ and $\hat{\alpha}_2$ meet but we do not enforce unification of the strong coupling constant $\hat{\alpha}_3$ with $\hat{\alpha}_{1,2}$ at $M_{\rm GUT}$. The experimental value of the $\overline{\rm MS}$ strong coupling constant at M_Z is an input in our scheme and this is related to $\hat{\alpha}_3$ through $\alpha_{\rm s}(M_Z) = \hat{\alpha}_3(M_Z)/(1 - \Delta\hat{\alpha}_3)$, where $\Delta\hat{\alpha}_3$ are the threshold corrections. Enforcing unification of $\hat{\alpha}_3$ with the rest of the gauge couplings usually results in values for $\alpha_{\rm s}(M_Z)$ larger than the experimental values, if the two- loop RGE's are used. For this reason we abandon gauge coupling unification. For the determination of the gauge couplings $\hat{\alpha}_{1,2}$ we use as inputs the electromagnetic coupling constant α_0, the value of the Fermi coupling constant $G_{\rm F}$, and the Z-boson mass M_Z. From these we determine the weak mixing angle through the relation

$$\hat{s}^2\hat{c}^2 = \frac{\pi\alpha_0}{\sqrt{2}M_Z^2 G_{\rm F}(1-\Delta\hat{r})} \,.$$

The value of the electromagnetic coupling constant at M_Z in the $\overline{\rm DR}$ scheme is calculated through $\hat{\alpha}(M_Z) = \alpha_0/(1 - \Delta\hat{\alpha}_{\rm em})$, where $\Delta\hat{\alpha}_{\rm em}$ are the appropriate threshold corrections (for details see [15]). In each iteration $\hat{s}^2$ and $\hat{\alpha}$ are extracted and from these the values of $\hat{\alpha}_{1,2}$ at M_Z are determined. In the equations above all hatted quantities are meant to be in the $\overline{\rm DR}$ scheme.

Our remaining inputs, in running the RGE's, are as usual the soft SUSY breaking parameters m_0, $M_{1/2}$, A_0, $\tan\beta$ and the sign of the parameter μ. The top and tau physical masses, M_t, M_τ, as well as the $\overline{\rm MS}$ bottom running mass $m_b(m_b)$ are also inputs. The default values for the aforementioned masses are $M_t = 175\,{\rm GeV}, M_\tau = 1.777\,{\rm GeV}$ and $m_b(m_b) = 4.25\,{\rm GeV}$. For the determination of the bottom and tau running masses, and hence their corresponding Yukawa couplings, at the scale M_Z, we run $SU_c(3) \times U_{\rm em}(1)$ RGE's using three-loop RGE's for the strong coupling constant. We also include two-loop contributions in the electromagnetic coupling and mixings of the electromagnetic with the strong coupling constant. The latter is as important as the three-loop strong coupling constant contribution to the RGE's. At the end of the running $\overline{\rm MS}$ masses are converted to $\overline{\rm DR}$ in the usual way. This determines the bottom and tau Yukawa couplings at M_Z. We recall that the corrections to the bottom Yukawa coupling of (2) should be duly taken into account. For the determination of the top Yukawa coupling at M_t we take into account all dominant corrections relating the pole to its running mass. By running the RGE's we can have the top Yukawa coupling at M_Z. Thus our analysis resembles that followed in [15].

For the determination of the Higgs and Higgsino mixing parameters, m_3^2 and μ, we solve the minimization conditions with the one-loop corrected effective potential in which all particle contributions are taken into account. The minimization is performed using as reference scale the average stop scale $Q_{\tilde{t}} \simeq (m_{\tilde{t}_1} m_{\tilde{t}_2})^{1/2}$. Thus in each run we determine $m_3^2(Q_{\tilde{t}}), \mu(Q_{\tilde{t}})$.

Regarding the calculation of the lightest supersymmetric particle (LSP) relic abundance, the Boltzmann equation is solved numerically using the machinery outlined in [2]. The coannihilation effects in regions where the right-handed stau, $\tilde{\tau}_{\rm R}$, approaches in mass the LSP are properly taken into account. Caution should be taken in regions where the ratio $m_A/2m_{\tilde{\chi}}$ is close to unity. This signals the vicinity of a pole in which case the traditional non-relativistic expansion breaks down. On the pole the annihilation cross section through the pseudo-scalar Higgs s-channel exchange is large and its width is important in determining its size. The rescaled pseudo-scalar Higgs boson width is $\Gamma_A/m_A \simeq 10^{-2}$, that is, it resembles that of the Z-boson, and hence for values of the ratio $m_A/2m_{\tilde{\chi}}$ larger than about 1.2 (see [21]) we are away from the pole region. We have found that in the $(m_0, M_{1/2})$ plane, and for both parameters less than 1 TeV, this ratio approaches unity only for the very large values of $\tan\beta > 50$. For such values of $\tan\beta$ the pseudo-scalar Higgs dominates the $\tilde{\chi}$ pair annihilation, leading to large cross sections and therefore cosmologically acceptable relic densities. Thus cosmologically allowed $m_0, M_{1/2}$ corridors open up for $\tan\beta > 50$ which were absent for lower values of $\tan\beta$. These are the same corridors observed in the analysis of [4] which however show up for lower values of $\tan\beta$.

In the panels shown in Fig. 2 we display our results by drawing the cosmologically allowed region $0.08 < \Omega_{\tilde{\chi}} h_0^2 < 0.18$ (dark green) in the $(m_0, M_{1/2})$ plane for values of $\tan\beta$ equal to 40, 45, 50 and 55 respectively. Also drawn (light green) is the region $0.18 < \Omega_{\tilde{\chi}} h_0^2 < 0.30$. In the figures shown the default values for the top, tau and bottom masses are assumed. The remaining inputs are shown on the top of each panel. The solid red mark the region within

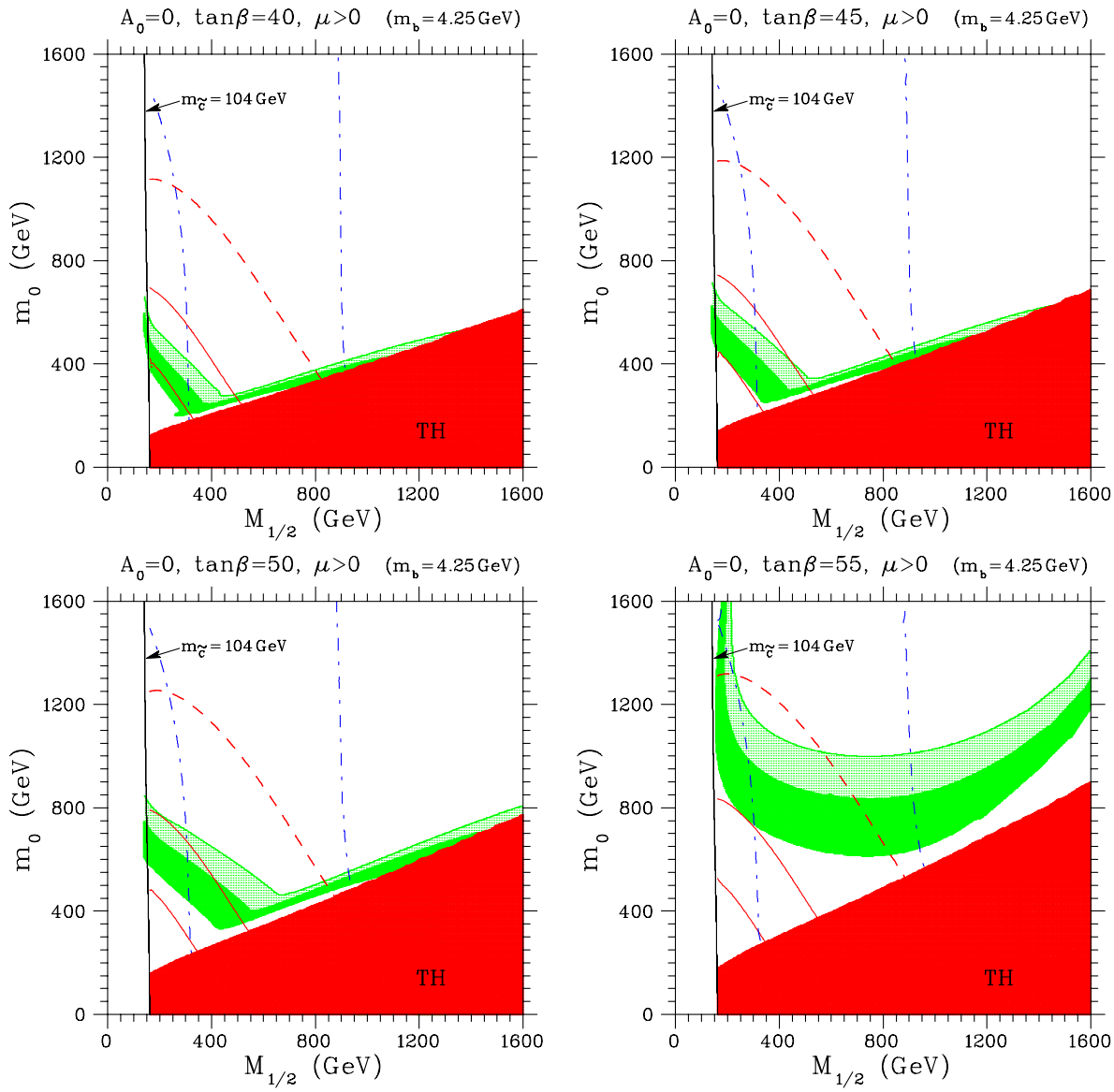

Fig. 2. Cosmologically allowed regions of the relic density for four different values of $\tan\beta$ in the $(M_{1/2}, m_0)$ plane. The remaining inputs are shown in each figure. The mass of the top is taken 175 GeV. In the dark green shaded area $0.08 < \Omega_{\tilde{\chi}} h_0^2 < 0.18$. In the light green shaded area $0.18 < \Omega_{\tilde{\chi}} h_0^2 < 0.30$. The solid red lines mark the region within which the supersymmetric contribution to the anomalous magnetic moment of the muon is $\alpha_\mu^{\rm SUSY} = (43.0 \pm 16.0) \times 10^{-10}$. The dashed red line is the boundary of the region for which the lower bound is moved to $11.2 < 10^{10} \alpha_\mu^{\rm SUSY}$. The dashed-dotted blue lines are the boundaries of the region $113.5\,{\rm GeV} \leq m_{\rm Higgs} \leq 117.0\,{\rm GeV}$

which the supersymmetric contribution to the anomalous magnetic moment of the muon falls within the E821 range $\alpha_\mu^{\rm SUSY} = (43.0 \pm 16.0) \times 10^{-10}$. The dashed red line marks the boundary of the region when the more relaxed lower bound $11.2 \times 10^{-10} \leq \alpha_\mu^{\rm SUSY}$ is used [9], corresponding to the 2σ lower bound of the E821 range. Along the blue dashed-dotted lines the light CP-even Higgs mass takes values 113.5 GeV (left) and 117.0 GeV (right) respectively. The line on the left marks therefore the recent LEP bound on the Higgs mass [12]. Also shown[2] is the chargino mass bound 104 GeV. The shaded area (in red) at the bottom of each figure, labelled by TH, is theoretically disallowed since the light stau is lighter than the lightest of the neutralinos. From the displayed figures we observe that for values of $\tan\beta$ up to 50 the cosmological data put an upper bound on the parameter m_0. However, there is practically no such upper bound for the parameter $M_{1/2}$, due to the coannihilation effects [4] which allow for $M_{1/2}$ as large as 1700 GeV within the narrow coan-

[2] In the context of our analysis focus point regions [3] show up for smaller values of the top mass. At this point we therefore agree with the findings of [4,6]. In any case the bulk of the focus point region appears for rather large values of m_0 and hence they are not favored by the $g-2$ data

Table 1. Upper bounds, in GeV, on the masses of the lightest of the neutralinos, charginos, staus, stops and Higgs bosons for various values of $\tan\beta$ if the E821 bounds are imposed. The values within brackets represent the same situation when the weaker bounds $11.2\times10^{-10} < \alpha_\mu^{\rm SUSY} < 59.0\times10^{-10}$ are used (see main text)

$\tan\beta$	$\tilde{\chi}^0$	$\tilde{\chi}^+$	$\tilde{\tau}$	$\tilde{t}$	h
10	108 (174)	184 (306)	132 (197)	376 (686)	115 (116)
20	154 (255)	268 (457)	175 (274)	603 (990)	116 (118)
30	191 (310)	338 (560)	212 (312)	740 (1200)	117 (118)
40	201 (340)	357 (617)	274 (353)	785 (1314)	117 (119)
50	208 (357)	371 (646)	440 (427)	822 (1357)	117 (119)
55	146 (311)	260 (563)	424 (676)	606 (1237)	115 (117)

nihilation band lying above the theoretically disallowed region. For $\tan\beta = 55$ a large region opens up within which the relic density is cosmologically allowed. This is due to the pair annihilation of the neutralinos through the pseudo-scalar Higgs exchange in the s-channel. As explained before, for such high $\tan\beta$ the ratio $m_A/2m_{\tilde{\chi}}$ approaches unity and the pseudo-scalar exchange dominates yielding large cross sections and hence small neutralino relic densities. In this case the lower bound put by the $g-2$ data cuts the cosmologically allowed region which would otherwise allow for very large values of $m_0, M_{1/2}$. The importance of these corridors has been stressed in the analysis of [4,6]. However, in our case these show up at much higher values of the parameter $\tan\beta$. We should remark at this point that in our analysis we use the value of $\alpha_{\rm strong}(M_Z)$ as input and relax unification of the α_3 gauge coupling with the others. For reasons already explained, in the constrained scenario it is almost impossible to reconcile gauge coupling unification with a value for $\alpha_{\rm strong}(M_Z)$ consistent with experiment due to the low energy threshold effects. This change drastically affects the values of other parameters and especially that of the Higgsino (μ) and Higgs (m_3^2) mixing parameters that in turn affect the pseudo-scalar Higgs boson mass which plays a dominant role. For the $\tan\beta = 55$ case, close to the highest possible value, and considering the conservative lower bound on the muon's anomalous magnetic moment $\alpha_\mu^{\rm SUSY} \geq 11.2\times10^{-10}$ and values of $\Omega_{\tilde{\chi}}h_0^2$ in the range 0.13 ± 0.05, we find that the point with the highest value of m_0 is (in GeV) at $(m_0, M_{1/2}) = (950, 300)$ and that with the highest value of $M_{1/2}$ is at $(m_0, M_{1/2}) = (600, 750)$. The latter marks the lower end of the line segment of the boundary $\alpha_\mu^{\rm SUSY} = 11.2\times10^{-10}$ which amputates the cosmologically allowed stripe. For the case displayed in the bottom right panel of Fig. 2 the upper mass limits put on the LSP, and the lightest of the charginos, stops and the staus are $m_{\tilde{\chi}} < 287$, $m_{\tilde{\chi}^+} < 539$, $m_{\tilde{t}} < 1161$, $m_{\tilde{\tau}} < 621$ (in GeV). Allowing for $A_0 \neq 0$ values, the upper bounds put on $m_0, M_{1/2}$ increase a little and so do the aforementioned bounds on the sparticle masses. Thus it appears that the prospects of discovering CMSSM at a e^+e^- collider with center of mass energy $s^{1/2} = 800\,$GeV, such as TESLA, are not guaranteed. However, in the allowed regions the next

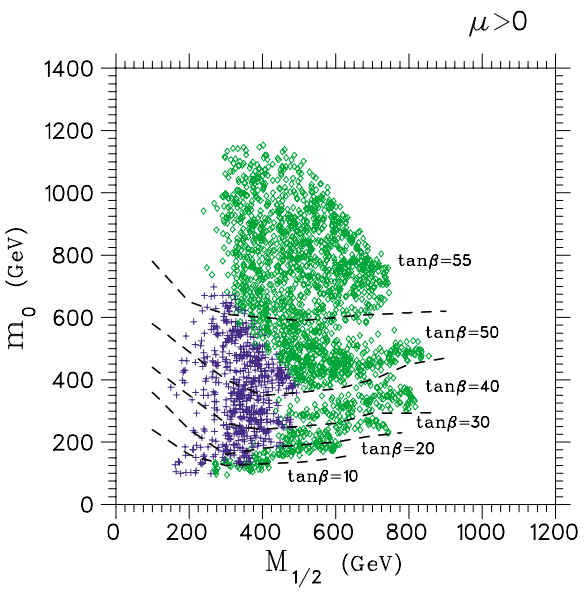

Fig. 3. In the $(M_{1/2}, m_0)$ plane, we display all points compatible with $\alpha_\mu^{\rm SUSY} = (43.0\pm16.0)\times10^{-10}$ (+) and $11.2\times10^{-10} < \alpha_\mu^{\rm SUSY} < 59.0\times10^{-10}$ ($\diamond$). All the points are consistent with the cosmological bound $\Omega_{\tilde{\chi}}h_0^2 = 0.13\pm0.05$ and they are grouped in regions, separated by dashed contours each of which is the boundary of $\tan\beta$ with the value shown beneath. In the top region, designated by $\tan\beta = 55$, the parameter $\tan\beta$ takes values between 50 and 55

to lightest neutralino, $\tilde{\chi}'$, has a mass very close to the lightest of the charginos and hence the process $e^+e^- \to \tilde{\chi}\tilde{\chi}'$, with $\tilde{\chi}'$ subsequently decaying to $\tilde{\chi} + l^+l^-$ or $\tilde{\chi} + 2$ jets, is kinematically allowed for such large $\tan\beta$, provided the energy is increased to at least $s^{1/2} = 900\,$GeV. It should be noted however that this channel proceeds via t-channel exchange of a selectron and is suppressed due to the heaviness of the exchanged sfermion.

The situation changes, however, when the strict E821 limits are imposed: $\alpha_\mu^{\rm SUSY} = (43.0\pm16.0)\times10^{-10}$. For instance in the $\tan\beta = 55$ case displayed in Fig. 2 there is no cosmologically allowed region which obeys this bound. For the other cases, $\tan\beta < 50$, the maximum allowed $M_{1/2}$ is about 475 GeV, occurring at $m_0 \simeq 375\,$GeV, and the maximum m_0 is 600 GeV when $M_{1/2} \simeq 300\,$GeV. The upper limits on the masses of the sparticles quoted previously reduce to $m_{\tilde{\chi}} < 192$, $m_{\tilde{\chi}^+} < 353$, $m_{\tilde{t}} < 775$, $m_{\tilde{\tau}} < 436$, all in GeV. However, these values refer to the limiting case $A_0 = 0$. Scanning the parameter space allowing also for $A_0 \neq 0$ we obtain the upper limits displayed in Table 1. In this table the unbracketed values correspond to the E821 limits on $g-2$. For completeness we also display, within brackets, the bounds obtained when the weaker lower bound $\alpha_\mu^{\rm SUSY} \geq 11.2\times10^{-10}$ is imposed. We see that even at TESLA with center of mass energy $s^{1/2} = 800\,$GeV, the prospects of discovering CMSSM are guaranteed in $e^+e^- \to \tilde{\chi}^+\tilde{\chi}^-$ if the E821 bounds are imposed.

In Fig. 3 we display in the $(M_{1/2}, m_0)$ plane the points which are consistent both with the muon's anomalous

magnetic moment bounds mentioned before and cosmology, as well as with the other accelerators data. Each of the points is taken from a sample of 40,000 random points in the part of the parameter space defined by $m_0 < 1.5\,\text{TeV}$, $M_{1/2} < 1.5\,\text{TeV}$, $|A_0| < 1\,\text{TeV}$ and $2 < \tan\beta < 55$. All the points are consistent with the cosmological bound $\Omega_{\tilde{\chi}} h_0^2 = 0.13 \pm 0.05$. The plus points (colored in blue) are those consistent with the E821 bound $27 \times 10^{-10} < \alpha_\mu^{\text{SUSY}} < 59 \times 10^{-10}$, while the diamonds (colored in green) are consistent with the more relaxed bound $11.2 \times 10^{-10} < \alpha_\mu^{\text{SUSY}} < 59 \times 10^{-10}$. The points are grouped in regions, separated by dashed contours, each of which constitutes the boundary of $\tan\beta$ with the value shown beneath. In the region designated as $\tan\beta = 55$ all points have $55 > \tan\beta > 50$. It is seen clearly that only a few points in the $\tan\beta > 50$ case can survive the E821 bound. For $\tan\beta < 50$ the parameter $M_{1/2}$ cannot be larger than about 500 GeV, attaining its maximum value at $m_0 \simeq 400\,\text{GeV}$, and the maximum m_0 is 725 GeV, occurring at $M_{1/2} \simeq 275\,\text{GeV}$. The upper limits put on $m_0, M_{1/2}$ result to the sparticle mass bounds displayed in Table 1.

4 Conclusions

In this work we have undertaken the problem of calculating the neutralino relic density in the framework of the CMSSM, by paying special attention to the pseudo-scalar Higgs exchange mechanism which is dominant in the large $\tan\beta$ region. Imposing the bounds $\alpha_\mu^{\text{SUSY}} = (43.0 \pm 16.0) \times 10^{-10}$ on the muon's anomalous magnetic moment, put by the BNL E821 experiment, in combination with the cosmological data $\Omega_{\tilde{\chi}} h_0^2 = 0.13 \pm 0.05$, severely restricts the sparticle spectrum. We found that the pseudo-scalar Higgs exchange mechanism opens cosmologically allowed corridors, of high $m_0, M_{1/2}$, only for the very large values $\tan\beta > 50$, which, however, have little overlap with the regions allowed by the E821 data. In fact only a few isolated points in the parameter space with $\tan\beta > 50$ can survive the restrictions imposed by both data. The bounds put on the sparticle spectrum can guarantee that in LHC but also in a e^+e^- linear collider with center of mass energy $s^{1/2} = 800\,\text{GeV}$, such as TESLA, CMSSM can be discovered. The guarantee for a TESLA machine with this energy is lost in a charged sparticle final state channel if the lower bound on the value of $g-2$ is lowered to its $\approx 2\sigma$ value, but not for the LHC. In this case only by increasing the center of mass energy to be $\simeq 1.2\,\text{TeV}$, a e^+e^- linear collider can find CMSSM in $\tilde{\tau}\tilde{\tau}^*$- or $\tilde{\chi}^+\tilde{\chi}^-$-channels.

Acknowledgements. A.B.L. acknowledges support from HPRN-CT-2000-00148 and HPRN-CT-2000-00149 programmes. He also thanks the University of Athens Research Committee for partially supporting this work. V.C.S. acknowledges support by a Marie Curie Fellowship of the EU programme IHP under contract HPMFCT-2000-00675. The authors thank D.V. Nanopoulos, H. Eberl, S. Kraml and W. Majerotto for valuable discussions.

References

1. M. Drees, M. Nojiri, Phys. Rev. D **47**, 376 (1993); R. Arnowitt, P. Nath, Phys. Lett. B **299**, 58 (1993)
2. A.B. Lahanas, D.V. Nanopoulos, V.C. Spanos, Phys. Rev. D **62**, 023515 (2000)
3. J.L. Feng, K.T. Matchev, F. Wilczek, Phys. Lett. B **482**, 388 (2000)
4. J. Ellis, T. Falk, G. Ganis, K.A. Olive, M. Srednicki, Phys. Lett. B **510**, 236 (2001)
5. H.N. Brown et al., Muon $g-2$ Collaboration, Phys. Rev. Lett. **86**, 2227 (2001)
6. J. Ellis, D.V. Nanopoulos, K.A. Olive, Phys. Lett. B **508**, 65 (2001)
7. L. Everett, G.L. Kane, S. Rigolin, L. Wang, Phys. Rev. Lett. **86**, 3484 (2001); J.L. Feng, K.T. Matchev, Phys. Rev. Lett. **86**, 3480 (2001); E.A. Baltz, P. Gondolo, Phys. Rev. Lett. **86**, 5004 (2001); U. Chattopadhyay, P. Nath, Phys. Rev. Lett. **86**, 5854 (2001); S. Komine, T. Moroi, M. Yamaguchi, Phys. Lett. B **506**, 93 (2001); J. Hisano, K. Tobe, Phys. Lett. B **510**, 197 (2001); R. Arnowitt, B. Dutta, B. Hu, Y. Santoso, Phys. Lett. B **505**, 177 (2001); K. Choi, K. Hwang, S.K. Kang, K.Y. Lee, W.Y. Song, Phys. Rev. D **64**, 055001 (2001); S.P. Martin, J.D. Wells, Phys. Rev. D **64**, 035003 (2001); S. Komine, T. Moroi, M. Yamaguchi, Phys. Lett. B **507**, 224 (2001); H. Baer, C. Balazs, J. Ferrandis, X. Tata, Phys. Rev. D **64**, 035004 (2001); V. Barger, C. Kao, Phys. Lett. B **518**, 117 (2001)
8. L. Roszkowski, R.R. Austri, T. Nihei, JHEP (2001) 0108024
9. S. Narison, Phys. Lett. B **513**, 53 (2001)
10. A.B. Lahanas, D.V. Nanopoulos, V.C. Spanos, Mod. Phys. Lett. A **16**, 1229 (2001)
11. M. Drees, Y.G. Kim, T. Kobayashi, M.M. Nojiri, Phys. Rev. D **63**, 115009 (2001)
12. Searches for the Neutral Higgs Bosons of the MSSM: Preliminary Combined Results Using LEP Data Collected at Energies up to 209 GeV, The ALEPH, DELPHI, L3 and OPAL coll., and the LEP Higgs Working Group, http://lephiggs.web.cern.ch/LEPHIGGS
13. B. de Carlos, J.A. Casas, Phys. Lett. B **309**, 320 (1993); H. Baer, C. Chen, M. Drees, F. Paige, X. Tata, Phys. Rev. Lett. **76**, 986 (1997); J.A. Casas, J.R. Espinosa, H.E. Haber, Nucl. Phys. B **526**, 3 (1998)
14. A. Katsikatsou, A.B. Lahanas, D.V. Nanopoulos, V.C. Spanos, Phys. Lett. B **501**, 69 (2001)
15. J.A. Bagger, K. Matchev, D.M. Pierce, R.-J. Zhang, Nucl. Phys. B **491**, 3 (1997)
16. R. Hempfling, Phys. Rev. D **49**, 6168 (1994); L.J. Hall, R. Rattazi, U. Sarid, Phys. Rev. D **50**, 7048 (1994); R. Rattazi, U. Sarid, Phys. Rev. D **53**, 1553 (1996)
17. M. Carena, M. Olechowski, S. Pokorski, C. Wagner, Nucl. Phys. B **426**, 269 (1994)
18. E. Accomando, R. Arnowitt, B. Dutta, Y. Santoso, Nucl. Phys. B **585**, 124 (2000)
19. H. Eberl, K. Hidaka, S. Kraml, W. Majerotto, Y. Yamada, Phys. Rev. D **62**, 055006 (2000)
20. M. Carena, D. Garcia, U. Nierste, C. Wagner, Nucl. Phys. B **577**, 88 (2000)
21. K. Griest, D. Seckel, Phys. Rev. D **43**, 3191 (1991)